

Nucleon–Pion States from $2 + 1 + 1$ -flavor Lattice QCD at Physical Pion Mass

Yong-Chull Jang^{1,*}

¹*Brookhaven National Laboratory, Physics Department, Upton, New York 11973*

(Dated: May 18, 2022)

The nucleon excited states which are supposed to be nucleon-pion states are extracted from the nucleon three-point correlator with the temporal component of the isovector axial current transferring nonzero momentum to the nucleon. This correlator shows a weak overlap with the ground state transition and strongly couples to the excited states which have been not accessible from the nucleon two-point correlators. Two-state description of nucleon reliably extracts the excited states, and the two levels from the entire spectrum are delicately chosen by pion exchanges. The smallness of the ground state transition might imply that the partially conserved axial current (PCAC) relation among axial form factors is manifested. The calculation is performed on the physical pion mass ensemble.

INTRODUCTION

The lattice QCD calculation of nucleon axial form factor G_A is important to provide inputs for upcoming high precision neutrino experiments with nuclear targets. Currently, the lattice results are higher than the experiments over the range of momentum transfer squared $Q^2 \lesssim 1.0 \text{ GeV}^2$. Thus, the axial charge radius, which is defined by the slope of the G_A with respect to Q^2 at zero, is smaller [1]. Lattice data also shows a large deviation, as approaching to the continuum and the chiral limit [2], from the PCAC relation among G_A and (induced) pseudoscalar (\tilde{G}_P) G_P form factors. There have been attempts to resolve the discrepancy by allowing different PCAC quark masses for nucleon two-point and three-point correlators with the axial current insertions [3], or by defining a projected current to suppress the excited states [4]. In both approaches, the induced pseudoscalar form factor results in much smaller value than the experiment at the muon capture scale. Chiral perturbation theory could explain the difference in the \tilde{G}_P by including nucleon-pion state corrections to the lattice results [5]. The lattice calculations, however, do not indicate the nucleon-pion state although the correlator fits include multiple exponentials to capture the excited states [6, 7].

Here, for the first time, the existence of the large number of nucleon-pion states is revealed from the three-point correlator with the temporal component of axial current, A_4 , transferring nonzero momentum between nucleon interpolating operators. The lowest level extracted is considered to be a two-particle $N\pi$ state. We used a $2 + 1 + 1$ -flavor HISQ ensemble generated by MILC collaboration [8] with lattice spacing $a \approx 0.09 \text{ fm}$, and the Clover valence quark is tuned to the unitary point $M_\pi \approx 138 \text{ MeV}$. More details about data and operator constructions can be found in Ref. [7].

The A_4 correlator has been commonly ignored from lattice calculations of the axial form factors. The main reason is that the correlator cannot be fitted, especially when the momentum transfer is small, with the ground

and excited states energies fixed by the nucleon two-point correlators. A possibility is that there are missing states extracted from two-point correlator, because the coupling is weak and thus the states are not resolved by fits. To explore the missing states from the A_4 correlators, first, the ground state energy from two-point correlators with the multistate fit is validated with Prony's method. Then, we relax the excited state energies, but keep the ground state energies frozen.

The excited state energies from the multistate fits have not been considered physically meaningful, because these are viewed as an effective quantity that grasps effects from all truncated states. Instead, lattice calculations of nucleon excited states have been performed by solving the generalized eigenvalue problem (GEVP) or by the variational approach [9–11]. However, the three-point function has not been solely explored for the spectroscopy, but for extracting hadronic matrix elements of lowest lying states to study hadron decays and structures. Here, it turns out that the A_4 current does couple weakly to the nucleon ground state transition unlike to the spatial components. Thus, the first excited state can be extracted cleanly, as in the usual situation that ground state can be extracted reliably when it dominates the correlators.

PRONY'S METHOD FOR TWO-POINT CORRELATORS

Results of the two-point correlator analysis from multistate fit [7] is revisited with a variant of the Prony's method [12] that results in generalized effective masses. First, two-point correlator fit including 2-state is performed for a shifted interval $[t_i, t_i + n - 1]$, keeping the number of data points $n = 6$. Generalized effective masses M_0 and M_1 give a better resolution of excited state effects than the conventional effective mass $m_{\text{eff}} = \ln[C(t)/C(t+1)]$ as shown in Fig. 1. The change in ground state energy M_0 is milder than in the m_{eff} , and the mass gap for the first excited state $\Delta M_1 = M_1 - M_0$

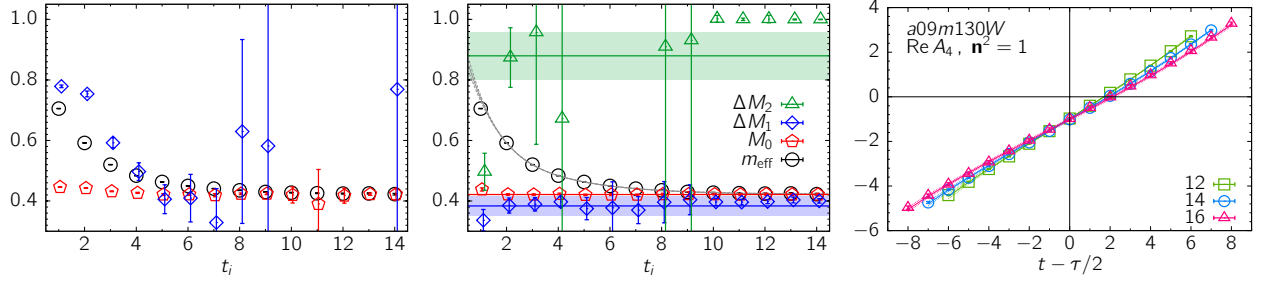


FIG. 1. Generalized effective masses from the Prony's method for the nucleon zero momentum two-point correlator with (left) 2-state and (middle) 3-state. The ΔM_2 for $t_i \geq 10$ is not moved away from the initial guess since the first two states saturate the correlator. The gray line represents m_{eff} calculated from the 3-state fit to the range $[2, 20]$ and the three bands are the results from the fit. (right) Data for the three-point correlator with A_4 current insertion. Curves with error represent the relaxed 2-state fit. Three source-sink separations are simultaneously fitted.

shows a plateau at $t_i \sim [5, 7]$ and loses the signal around $t_i = 8$.

Having plateau for M_0 and ΔM_1 , the procedure is repeated with 3-state fit with priors $\Delta M_1 = 0.4(1)$ as well as $M_0 = 0.42(1)$ to prevent a numerical instability. Then, masses M_0 and M_1 become stable from $t_i = 2$ and the signal for the third state is so weak from $t_i = 3$ that the plateau for $\Delta M_2 = M_2 - M_0$ is unclear. The ΔM_2 from the fit with $t_i = 1$ has a small error but is vetoed, because of the large $\chi^2/\text{d.o.f.}$

Lastly, 3-state fit with the fit range $[2, 20]$ is performed. The results are consistent with the 3-state Prony's method, and the M_0 and M_1 are consistent with the 4-state fit result in Ref. [7] although the remnants are captured differently by the higher excited states in the 3- and 4-state fits. For the main results in this paper, we only need the ground state parameters, which are almost identical for all variations mentioned above for all momenta.

NUCLEON SPECTRUM FROM AXIAL CURRENT A_4 THREE-POINT CORRELATORS

Spectral decomposition of the three-point correlator is given as follows.

$$\begin{aligned}
 C[A_4(\mathbf{p}', t)](\tau) &= \sum_{i,j} |\mathcal{A}'_i| |\mathcal{A}_i| \mathcal{M}_{i'j} e^{-E_i t - M_j(\tau-t)} \\
 &= |\mathcal{A}'_0| |\mathcal{A}_0| (\mathcal{M}_{0'0} e^{-E_0 t - M_0(\tau-t)} + r'_1 r_1 \mathcal{M}_{1'1} e^{-E_1 t - M_1(\tau-t)} \\
 &\quad + r_1 \mathcal{M}_{0'1} e^{-E_0 t - M_1(\tau-t)} + r'_1 \mathcal{M}_{1'0} e^{-E_1 t - M_0(\tau-t)} \\
 &\quad + \dots), \tag{1}
 \end{aligned}$$

where the final states have momentum $\mathbf{p}' = 2\pi\mathbf{n}/L$, energy E_i and the initial state at rest has mass M_j .

In previous studies, the multistate fits given in Eq. (1) take final (initial) states amplitude $|\mathcal{A}'_i|$ ($|\mathcal{A}_j|$), E_i and M_j from two-point correlator fits. Thus, only the matrix elements $\mathcal{M}_{i'j} \equiv \langle i' | A_4 | j \rangle$ are free parameters. Typically,

as the momentum transfer becomes smaller, the fits become worse. For $\mathbf{n}^2 = 1$, $\chi^2/\text{d.o.f.} \sim 22$. The pooriness of the fit does not depend much on whether the two-point correlator fit parameters are taken from the 3-state or 4-state fit.

Here, the excited state parameters in the 2-state fit of three-point A_4 correlators are relaxed to be free, and the fit takes only the ground state properties from two-point correlator fit. Then, fit parameters are energy and mass gaps, $E_1 - E_0$ and $M_1 - M_0$, and $\mathcal{M}_{0'0}$, $r_1 \mathcal{M}_{0'1}$, $r'_1 \mathcal{M}_{1'0}$, $r'_1 r_1 \mathcal{M}_{1'1}$. Thus, the matrix elements involving the excited states, which are not a primary interest in the study of nucleon structures – e.g., form factors, can no longer be separated. The relaxed 2-state fit describes the data very well as shown in Fig. 1 and extracts the excited state parameters reliably as given in Table II and Fig. 2. For $\mathbf{n}^2 = 1$, $\chi^2/\text{d.o.f.} = 0.689$, $p = 0.76$, and other fits to momentum transfer up to $\mathbf{n}^2 = 6$ are significantly improved as shown in Table III. Note that only the data satisfying $t - \tau/2 \geq 0$ and $\tau \geq 12$ are included in the fit to avoid complications with fit interval and to stay away from a possible third state and beyond at the source $t = 0$ with energy E_i . And, two points are further omitted from the sink at $t = \tau$. The rest of the data points are well predicted by the relaxed 2-state fit curve in Fig. 1. Without losing the discussions, we proceed without including more data points from the left half side of the correlator.

The first excited states $1'$ and 1 , from Fig. 2, are not connected by the Lorentz boost: $M_1 > E_1$. The rest mass for the boosted state $1'$ is obtained by $M'_1 = \sqrt{E_1^2 - E_0^2 + M_0^2}$. Here, we used $E_0^2 - M_0^2$ in place of \mathbf{p}'^2 to propagate the correlations, which is justified because the ground states spectrum, M_0 and E_0 , follows the relativistic dispersion relation within a few percent. Then, we have an access to the ample spectrum of nucleon excited states $M_1^{(\prime)}$, which is supposed to be various nucleon-pion states as expected for the physical pion mass ensembles.

The mass differences $\Delta M_1^{(\prime)} = M_1^{(\prime)} - M_0$ of the excited nucleon-pion states $M_1^{(\prime)}$ from the ground nucleon

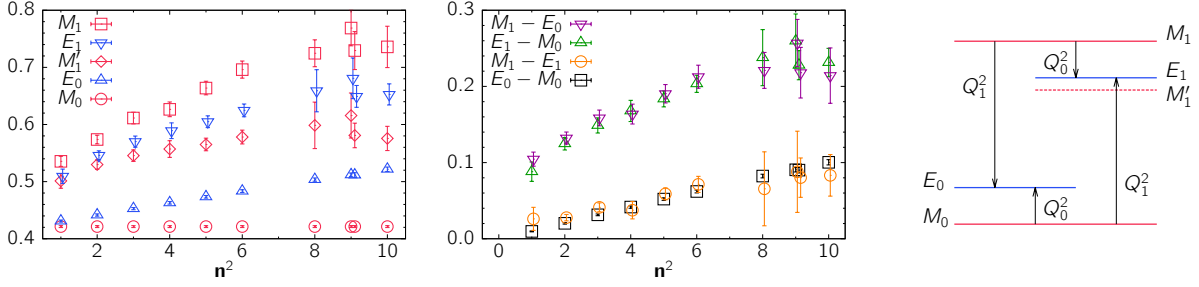


FIG. 2. The fit parameters $E_1 - E_0$ and $M_1 - M_0$ of the relaxed 2-state fits are converted into (left) the spectrum and (middle) exponents in Eq. (1). (right) The structure of spectrum accessed at fixed n^2 .

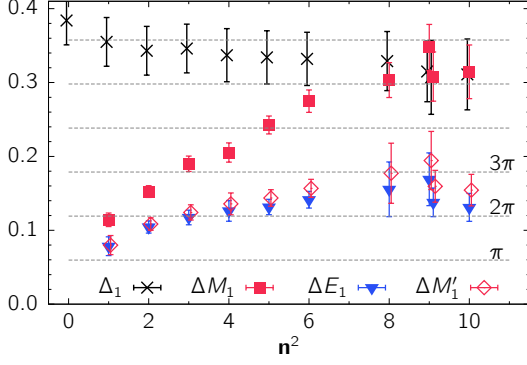


FIG. 3. Mass and Energy gaps from the ground states. $\Delta_1(n^2) = E_1^{2\text{pt}} - E_0$, where $E_1^{2\text{pt}}$ is taken from the two-point correlator fit.

TABLE I. The states are labeled by indicating the closest lower bound of $M_N + nM_\pi$. The $\Delta M'_1$ at $n^2 = 4$ is ambiguous and thus not classified. The values are given in lattice unit.

	$n^2 : \Delta M_1$	$n^2 : \Delta M'_1$	
$N\pi$		1: 0.080(13)	
$(N\pi\pi)_1$	1: 0.114(09)	2: 0.108(08)	3: 0.124(10)
$(N\pi\pi)_2$	2: 0.152(08)	5: 0.144(11)	6: 0.157(12)

state M_0 are plotted in Fig. 3 as well as the energy difference $\Delta E_1 = E_1 - E_0$. Note that $\Delta E_1 \lesssim \Delta M'_1$, which is expected when the states are boosted. Within this approach, it is hard to assign detailed properties such as the orbital and radial excitations to the extracted nucleon-pion states. However, the lowest level, which is accessed via M'_1 at $n^2 = 1$, lying closely above $M_N + M_\pi$, can be identified with a two particle $N\pi$ state, possibly with the positive parity according to the nucleon interpolating operator. A result for the negative parity $N\pi$ state in S-wave was obtained from the GEVP study using a $N_f = 2$ Clover fermions with $M_\pi \approx 160$ MeV, $a \approx 0.073$ fm, and $M_\pi L \sim 2.8$ [9], where the mass is similar to the lowest level in Fig. 3. Restricted to the $n^2 \leq 6$ probes, two independent determinations of mass splittings, ΔM_1 and $\Delta M'_1$, from different momentum probes show overlaps. It could be useful for cross-validation and for classifying

several results as two levels $(N\pi\pi)_1$ and $(N\pi\pi)_2$ as given in Table I.

TABLE II. Matrix elements $\mathcal{M}_{i'j}$ are given in terms of the fit parameters in Eq. (1).

n^2	$\mathcal{M}_{0'0}$	$r_1 \mathcal{M}_{0'1}$	$r'_1 \mathcal{M}_{1'0}$	$r'_1 r_1 \mathcal{M}_{1'1}$
1	$3.35(7.62) \times 10^{-1}$	4.18(59)	-6.41(67)	1.84(82)
2	$-0.27(1.39) \times 10^{-2}$	3.18(14)	-4.36(08)	0.75(42)
3	$-2.11(8.88) \times 10^{-3}$	2.46(12)	-3.49(08)	0.73(46)
4	$-0.28(1.08) \times 10^{-1}$	2.11(13)	-2.90(12)	0.24(52)
5	$-0.39(1.67) \times 10^{-2}$	1.71(09)	-2.55(08)	0.63(43)
6	$-1.30(4.06) \times 10^{-3}$	1.40(10)	-2.31(09)	0.94(52)
8	$-1.05(1.94) \times 10^{-1}$	1.15(15)	-1.71(13)	0.69(55)
9	$-0.58(1.64) \times 10^{-1}$	0.95(15)	-1.74(13)	1.31(68)
9'	$-0.84(3.27) \times 10^{-3}$	1.04(16)	-1.60(12)	0.29(83)
10	$-0.75(3.13) \times 10^{-3}$	0.87(17)	-1.46(10)	0.71(80)

TABLE III. The goodness of the fits to $C[A_4]$. The 3* fits are taken from the analysis presented in [6, 7].

n^2	relaxed 2-state		3*-state	
	$\chi^2/\text{d.o.f}$	p	$\chi^2/\text{d.o.f}$	p
1	0.698	0.76	21.78	$< 5 \times 10^{-5}$
2	1.654	0.06	19.36	$< 5 \times 10^{-5}$
3	2.018	0.02	11.79	$< 5 \times 10^{-5}$
4	1.086	0.37	4.757	$< 5 \times 10^{-5}$
5	2.066	0.01	5.348	$< 5 \times 10^{-5}$
6	2.067	0.02	4.834	$< 5 \times 10^{-5}$
8	1.054	0.40	1.724	0.03
9	2.247	0.01	2.726	0.001
9'	0.698	0.77	0.974	0.49
10	0.750	0.70	1.089	0.35

π -TOPIA

From Table II, the ground state matrix element $\mathcal{M}_{0'0}$ is zero within errors and the $\mathcal{M}_{1'1}$ is marginally determined. The smallness of the ground states matrix element $\mathcal{M}_{0'0}$ is crucial. Because the $0 \rightarrow 0'$ transition is faint, the first excited states are reliably ex-

tracted as they become in effect the ground states of the correlator $C[A_4]$. Note that the dependence in current insertion time t at fixed source-sink separation τ is given by $e^{(M_j - E_i)t}$ for each contribution in Eq. (1). The four exponents are shown in Fig. 2. Note that $-(M_0 - E_0) \simeq M_1 - E_1 < -(M_0 - E_1) \simeq M_1 - E_0$. Then, signal for the transition between ground states $0 \rightarrow 0'$ exponentially decays, while the $1 \rightarrow 1'$ for the first excited states is growing reciprocally faster than $0 \rightarrow 0'$. Similarly, $1 \rightarrow 0'$ is exponentially growing and $0 \rightarrow 1'$ decays even faster than $0 \rightarrow 0'$. Thus, the exponential rate of changes could partially explain that $\mathcal{M}_{0'0}$ is poorly determined than $\mathcal{M}_{1'1}$, because $\mathcal{M}_{1'0}$ is well determined though it is associated with faster decaying exponential.

There could be a strong underlying symmetry and kinematic relations that automatically pick the $0 \rightarrow 1'$ transition by the fastest growing signal of $1 \rightarrow 0'$ that stands out from the data in Fig. 1. The transition pattern and splittings depicted in Fig. 2 can be explained by the effective nucleon-pion interaction. Considering kinematics, if two transitions absorb a pion π^\pm with $Q_i^2 = \mathbf{p}^2 - (E_i - M_0)^2$, $i = 0, 1$, there must be two transitions that emit anti-pion π^\mp at the same Q_i^2 . Thus, the strong signal $1 \rightarrow 0'$ induces $0 \rightarrow 1'$ by the realization of particle-antiparticle symmetry. Although the $0 \rightarrow 0'$ signal is also decaying in time, M_0 and E_0 are provided externally from the two-point correlator, and thus the transition gap is well determined to form a firm constraint that induces $1 \rightarrow 1'$ transition. The pattern can be successively applied. For example, $M_1(\mathbf{n}^2 = 1) \sim M'_1(\mathbf{n}^2 = 2)$ in Fig. 2. Boost of M_0 and M'_1 at $\mathbf{n}^2 = 2$ forms inner levels E_0, E_1 in Fig. 2. Then, the full pion exchanges are allowed by completing the outer level M_1 . It is consistent with the identifications of $(N\pi\pi)_1$ and $(N\pi\pi)_2$ in Table I. By applying the induction reversely, the $M'_1(\mathbf{n}^2 = 1)$ is the lowest excited state at the zero momentum transfer, because inner levels E_0 and E_1 do not exist. Thus, it could be useful to improve the systematics in the axial charge g_A calculation with spacial components of axial current, and lacking the A_4 correlator at zero momentum $\mathbf{n}^2 = 0$ is not a concern for obtaining the $N\pi$ state in Table I.

The effective nucleon-pion interaction, which explains the extracted spectrum of nucleon-pion states, is a leading contribution of the induced pseudoscalar form factor, i.e., pion-pole dominance $\tilde{G}_P(Q^2) = [4M_N^2/(Q^2 + M_\pi^2)]G_A(Q^2)$ [2]. Note that the ground state matrix element relates the two form factors $\mathcal{M}_{0'0} = ((M_0 - E_0)/2M_0)\tilde{G}_P + G_A$ up to overall kinematic factor of $\mathcal{O}(1)$. From Fig. 2, $1/(E_0 - M_0)$ diverges as the momentum decreases. Interestingly, the divergence is very close to the pion-pole dominance factor so that $(E_0 - M_0)/2M_0 \times [4M_0^2/(Q^2 + M_\pi^2)] \simeq 1$ numerically for the physical ensemble analyzed. For the large momentum $\mathbf{n}^2 \geq 4$, the deviation from 1 is about 5% or less, and for the small momentum, the maximum deviation is 15% lower than

1 at $\mathbf{n}^2 = 1$. Considering that $\mathcal{M}_{0'0}$ is ill-determined, the correction to the pion-pole dominance ansatz could enter in a way that the cancellation of the two divergences becomes larger. Thus, the weak contribution of $\mathcal{M}_{0'0}$ could indicate a manifesting PCAC relation or the axial Ward identity in lattice calculations. Note that the PCAC relation $2m_q G_P = 2M_N G_A - (Q^2/2M_N)\tilde{G}_P$ reduces to the pion-pole dominance ansatz provided $2m_q G_P = (M_\pi^2/2M_N)\tilde{G}_P$, where the m_q is the PCAC quark mass [2].

CONCLUSION

The first excited states extracted from the nucleon three-point correlator $C[A_4]$ with the temporal component of the axial current are different from the excited states coupled to the two-point correlator, and the lowest lying state has mass of $N\pi$ state. The underlying pion absorption and emission are delicately paired by particle-antiparticle symmetry so that the discrete spectrum of the nucleon excitations which are considered as nucleon-pion states on the lattice emerges. Probes with different momentum transfers, as in the spectroscopy experiment, can collectively draw the structure of the spectrum.

The pion exchanges could be consistently described by the pion-pole dominance ansatz of the induced pseudoscalar form factor \tilde{G}_P . The pion-pole divergence is significantly cancelled by the kinematic factor, which determines the relative weight of \tilde{G}_P and axial form factor G_A in the ground state matrix elements $\mathcal{M}_{0'0}$ of $C[A_4]$. The cancellation can make the $\mathcal{M}_{0'0}$ contribution faint, thus the first excited state can be reliably determined. The smallness of $\mathcal{M}_{0'0}$ extracted from the data might imply that the PCAC relation, from which the pion-pole dominance can be derived, is manifested in the lattice calculations. The persistent discrepancy with the PCAC relation in lattice calculations might originate from the first excited state extracted from the two-point correlator, which has large mass that omits many nucleon-pion states in Fig. 3. Thus, systematics in the extraction of axial and (induced) pseudoscalar form factors could be improved by including the nucleon-pion states obtained from the three-point correlator $C[A_4]$.

ACKNOWLEDGEMENT

The author is grateful to R. Gupta and T. Bhattacharya for fruitful discussions. The author is also grateful to C. Jung for his help in manuscript preparation. We thank the MILC Collaboration for providing the 2+1+1-flavor HISQ lattices. The calculations used the Chroma software suite [13]. Simulations were carried out on computer facilities of (i) the National Energy Research Scientific Computing Center, a DOE Office of Science User

Facility supported by the Office of Science of the U.S. Department of Energy under Contract No. DE-AC02-05CH11231; and, (ii) the Oak Ridge Leadership Computing Facility at the Oak Ridge National Laboratory, which is supported by the Office of Science of the U.S. Department of Energy under Contract No. DE-AC05-00OR22725; (iii) the USQCD Collaboration, which are funded by the Office of Science of the U.S. Department of Energy, and (iv) Institutional Computing at Los Alamos National Laboratory. Y.-C. Jang was partly supported by the LANL LDRD program and is supported by the Exascale Computing Project (17-SC-20-SC), a collaborative effort of the U.S. Department of Energy Office of Science and the National Nuclear Security Administration.

* ypj@bnl.gov

- [1] R. J. Hill, P. Kammel, W. J. Marciano, and A. Sirlin, Rept. Prog. Phys. **81**, 096301 (2018), arXiv:1708.08462 [hep-ph].
- [2] R. Gupta, Y.-C. Jang, H.-W. Lin, B. Yoon, and T. Bhattacharya, Phys. Rev. **D96**, 114503 (2017), arXiv:1705.06834 [hep-lat].
- [3] K.-I. Ishikawa, Y. Kuramashi, S. Sasaki, N. Tsukamoto, A. Ukawa, and T. Yamazaki (PACS), Phys. Rev. **D98**, 074510 (2018), arXiv:1807.03974 [hep-lat].
- [4] G. S. Bali, S. Collins, M. Gruber, A. Schfer, P. Wein, and T. Wurm, Phys. Lett. **B789**, 666 (2019), arXiv:1810.05569 [hep-lat].
- [5] O. Bar, in *36th International Symposium on Lattice Field Theory (Lattice 2018) East Lansing, MI, United States, July 22-28, 2018* (2018) arXiv:1808.08738 [hep-lat].
- [6] Y.-C. Jang, T. Bhattacharya, R. Gupta, H.-W. Lin, and B. Yoon, *36th International Symposium on Lattice Field Theory (Lattice 2018) East Lansing, MI, United States, July 22-28, 2018*, PoS **LATTICE2018**, 123 (2018), arXiv:1901.00060 [hep-lat].
- [7] R. Gupta, Y.-C. Jang, B. Yoon, H.-W. Lin, V. Cirigliano, and T. Bhattacharya, Phys. Rev. **D98**, 034503 (2018), arXiv:1806.09006 [hep-lat].
- [8] A. Bazavov *et al.*, Phys. Rev. **D87**, 054505 (2013), arXiv:1212.4768 [hep-lat].
- [9] C. Alexandrou, T. Korzec, G. Koutsou, and T. Leontiou, Phys. Rev. **D89**, 034502 (2014), arXiv:1302.4410 [hep-lat].
- [10] C. B. Lang and V. Verduci, *Proceedings, 9th International Workshop on the Physics of Excited Nucleons (NSTAR 2013): Valencia, Spain, May 27-30, 2013*, Int. J. Mod. Phys. Conf. Ser. **26**, 1460056 (2014), arXiv:1309.4677 [hep-lat].
- [11] R. G. Edwards, J. J. Dudek, D. G. Richards, and S. J. Wallace, Phys. Rev. **D84**, 074508 (2011), arXiv:1104.5152 [hep-ph].
- [12] G. T. Fleming, S. D. Cohen, H.-W. Lin, and V. Pereyra, Phys. Rev. **D80**, 074506 (2009), arXiv:0903.2314 [hep-lat].
- [13] R. G. Edwards and B. Joo (SciDAC Collaboration, LHPC Collaboration, UKQCD Collaboration), Nucl.Phys.Proc.Suppl. **140**, 832 (2005), arXiv:hep-lat/0409003 [hep-lat].